Progress In Electromagnetics Research, PIER 69, 219–226, 2007

SHARP-REJECTION LOW-PASS FILTER WITH CONTROLLABLE TRANSMISSION ZERO USING COMPLEMENTARY SPLIT RING RESONATORS (CSRRS)

J. Zhang, B. Cui, S. Lin, and X.-W. Sun †

Shanghai Institute of Microsystem & Information Technology, CAS
Shanghai 200050, China

Abstract—A novel low-pass filter using complementary split ring resonators (CSRRs) for transmission zero control and sharp-rejection is presented. Three different CSRRs resonators cells are etched at the ground plane below a low impedance microstrip line for transmission zero control. A demonstration lowpass filter is designed, fabricated and measured. It agreed with the simulated results well.

1. INTRODUCTION

Low-pass filters (LPFs) of high quality, compact size and flexible reconfiguration are always desirable in modern microwave communication systems to remove undesired harmonics or spurious mixing products. Compact microstrip resonator cell (CMRC) [1] and defected ground structure (DGS) [2, 3], as well as stepped impedance resonators (SIRs) are commonly used for this purpose. In the practice application, one of the requisite qualities is sharp pass-band to stop-band transition. But, the filters mentioned above all have gradual cut-off response. The rejection characteristic can be improved by increasing the number of cascade sections, which, however, would unfortunately deteriorate pass-band insertion loss (IL) and lead to larger physical size of the filter.

Recently, complementary spilt ring resonators (CSRRs) as the negative image of a split ring resonators (SRRs) have been investigated for negative permittivity and left handed (LH) metamaterial in planar configuration [4–6]. The dominant driving mechanism for CSRRs excitation is electric coupling, the electric field must be applied in

† The authors are also with Graduate School of the Chinese Academy of Sciences, China.

the axial direction. For CSRR based transmission lines CSRRs must be etched either in the conductor strip or in the ground plane, in that region where the electric field is maximal.

The slow-wave factor of the microstrip line with CSRRs cells is defined by $\sqrt{\varepsilon_{eff,d}}$ and given as follows:

$$\sqrt{\varepsilon_{eff,d}} = \frac{\lambda_0 \Delta\theta}{360L} + \sqrt{\varepsilon_{eff}}$$

with

$$\varepsilon_{eff} = \frac{\varepsilon_r + 1}{2} + \frac{\varepsilon_r - 1}{2}\left(1 + 12\frac{h}{w}\right)^{-0.5}$$

where L is the physical length of microstrip line, λ_0 is the guided wavelength, and $\Delta\theta$ is the phase difference (in degrees) of microstrip lines between with and without CSRRs. ε_{eff} is the effective microstrip permittivity.

Figure 1 shows the variation of the slow- wave factor in terms of the effective permittivity with frequency. It can be seen that the uniform microstrip line shows an slow-wave factor of 1.48 in all frequency, where the proposed CSRRs microstrip line increased the slow-wave factor to 1.85 at the frequency 5.8 GHz, The results reveal that the slow-wave factors of the CSRRs microstrip line are improved by CSRRs cell, which also means the geometry size reduction.

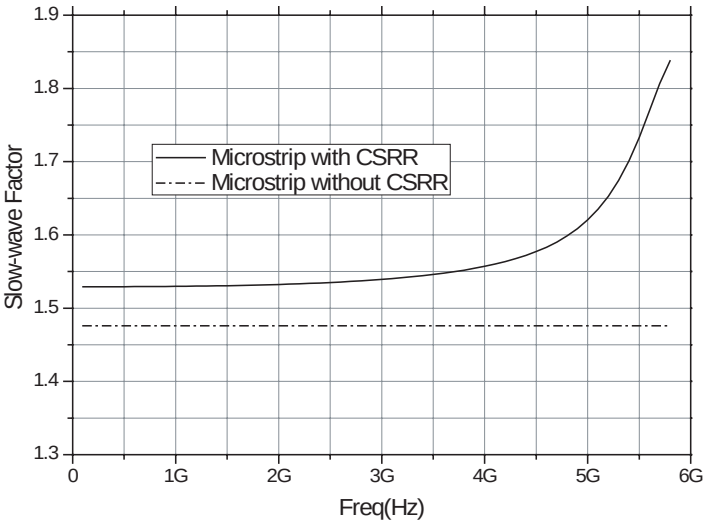

Figure 1. The slow-wave factor comparison with CSRRs and uniform microstrip line.

In the paper [7], CSRRs were used to design low-pass filter (LPF) for the first time, but an open stub as a capacitive load was still used to eliminate spurious response, which, however, induce larger circuit dimension.

Here, an improved LPF is proposed using multi-CSRR cells cascaded. By changing the radius and line width of CSRR, a set of gradual transmission zero can be got. In this letter, the presented LPF is realized by cascading three CSRR cells to obtain three controllable transmission zeroes. With transmission zero appropriately chosen, the stop-band range of the filter could be expanded; meanwhile the sharp-rejection of pass-band to stop-band transition could be still maintained. The proposed one has been designed, fabricated, and measured on the substrate of $\varepsilon_r = 2.65$, thickness $h = 254\,\mu$m and loss tangent of 0.003. It shows good response with the simulated performance.

2. DESIGN

Figure 2 shows the CSRR cell etched in the ground plane and the microstrip on the surface located between two $50\,\Omega$ line. The proposed LPF has a much wider microstrip line than conventional microstrip LPF, and does not include high impedance lines, which have been essentially required in conventional design. The wide transmission line on the surface just above the etched CSRR cell on the ground plane is applied as a compensated shunt capacitance which is usually realized by open stub. Therefore, no discontinuity elements such as tee- junction or cross-junction for connecting open stubs are required in the proposed LPF topology.

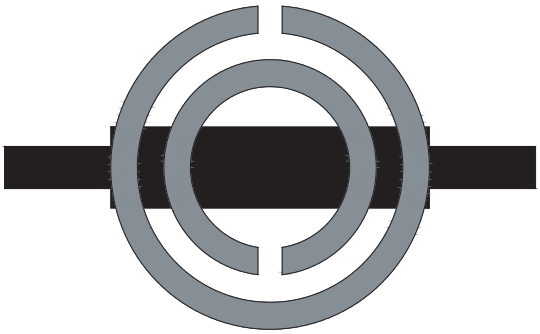

Figure 2. Topology of the CSRR (The upper metallization is depicted in black, whereas the bottom metal regions are depicted in grey).

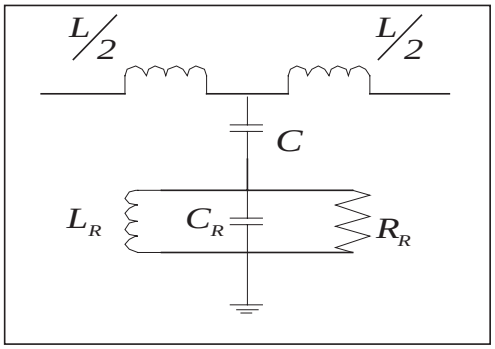

Figure 3. Equivalent lumped parameter circuit of CSRR.

The corresponding equivalent lumped circuit of the CSRR model has been reported in [8], but it has been reproduced here for clarity and completeness. In the model, L is the line inductance, C is the coupling capacitance between the line and the CSRR. The resonator is described by means of a parallel tank, C_R and L_R being the reactive elements and R_R accounting for losses.

Figure 4 describes the simulated frequency response of the basic CSRR cell with different CSRR design parameters. Table 1 and

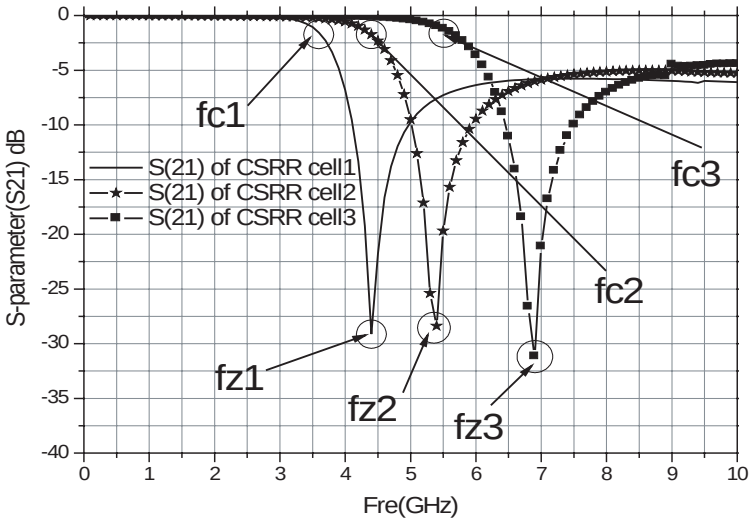

Figure 4. Simulated frequency response of basic CSRR cell with different CSRR design parameter.

Table 1. Geometry dimension of CSRR cell.

	r (mm)	c (mm)	d (mm)	w (mm)
CSRR1	3	0.5	0.5	0.5
CSRR2	2.5	0.4	0.4	0.4
CSRR3	2	0.3	0.3	0.3

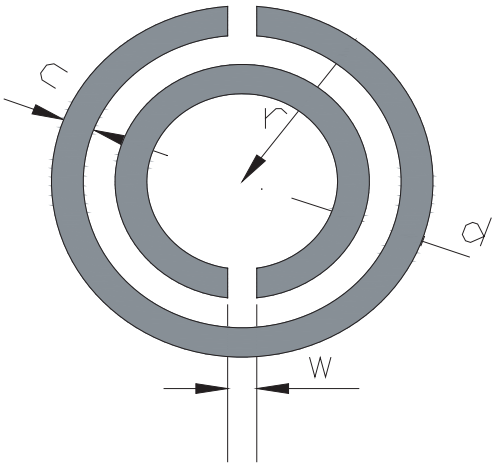

Figure 5. Geometry dimension of CSRR cell.

Figure 5 list the parameter configuration. If transmission zero frequency (f_Z) which nulls the shunt impedance is defined as

$$f_z = \frac{1}{2\pi\sqrt{L_R\left(C_R + C\right)}}$$

It can be clearly found that $f_{3\text{dB}}$ is immediately close to f_Z, which means a sharp rejection from pass-band to stop-band. However, the increase of the magnitude of the transmission response against frequency on the upper f_Z range band can also be noticed, which leads to a spurious pass band. If we alter the geometry parameters of CSRR cell by decreasing the radius r of the circle and width c of ring and split gap w, $f_{3\text{dB}}$ and f_Z of the CSRR cell increase drastically. Therefore, choosing geometry dimension of CSRR cell appropriately, $f_{3\text{dB}}$ and f_Z of the transmission response could be tuned into an arbitrary frequency range.

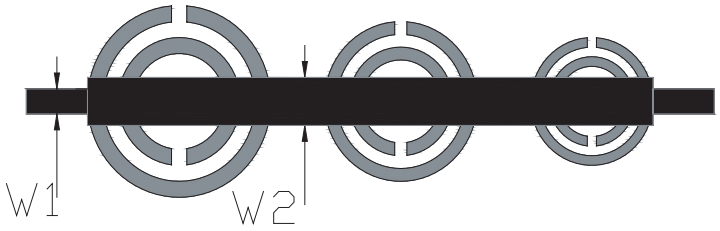

Figure 6. Layout of the proposed low-pass filter (LPF).

Figure 6 shows the layout of the proposed low-pass filter. It consists of three different CSRR cells, which are cascaded with low impedance transmission lines. The geometry and electric characteristic of the cells are detailed in the Table 1 and Figure 5 respectively. In the proposed filter, the transmission zero of the CSRR cells were adjusted at 4.4 GHz, 5.4 GHz, 6.9 GHz respectively, which can be designed by tuning the geometry parameter. In the process of design, the variation of the r, c, d, w against the C_R and L_R can be easily applied to determine the transmission zero f_Z. The final result are verified by EM simulator Ansoft HFSS. Because of the high Q value of the CSRR intrinsic LC tanker, the spurious pass band occurs rapidly on the upper f_Z frequency range. Therefore, we cascade the different CSRR cells to tune their transmission zeros into the stop-band frequency range of the filter and put the spurious pass-band to upper frequency.

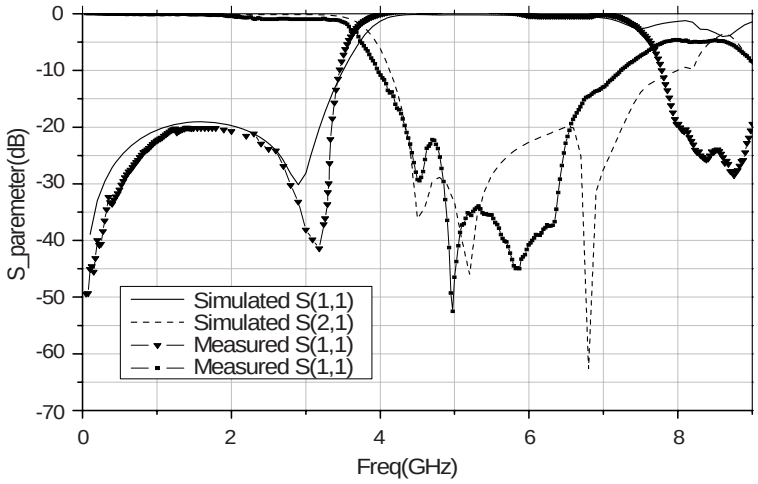

Figure 7. Simulated and measured result of the proposed LPF.

3. MEASURED AND SIMULATED RESULTS

The proposed low-pass filter was designed, fabricated and measured with the line width $W1 = 780\,\mu$m and $W2 = 1500\,\mu$m. $W1$ is the $50\,\Omega$ microstrip line width, $W2$ is the $30\,\Omega$ low impedance microstrip line width. The geometry dimensions of the CSRR cells are depicted in the Table 1. Measurements have been done using HP8510C vector network analyzer. The simulated and measured results are shown in the Figure 7.

The insert loss below 2.2 G is less than 0.9 dB, the return loss in pass-band is better than −20 dB. The 20 dB stop-band width is from 4.3 G to 6.5 G. Measured zero1 and zero2 agree with the simulated well while zero3 deflected from the simulated one to lower frequency due to the fabrication tolerance and the increase of radiation against the frequency at the CSRRs section. Figure 8 shows the photography of the proposed LPF.

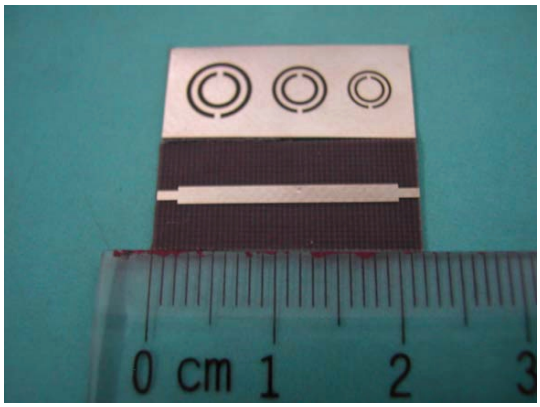

Figure 8. Photography of the proposed lowpass filter.

4. CONCLUSION

A novel microstrip lowpass filter using CSRRs is proposed. The lowpass filter is not only of good performance, low insertion loss, Sharp-rejection from passband to stopband but also has a wide stop-band owing to controllable transmission zero t by CSRRs cells. It can be easily implemented in microwave integrated circuit.

REFERENCES

1. Gu, J. and X. Sun, "Compact lowpass filter using spiral compact microstrip resonant cells," *Electronic Letters*, Vol. 41, No. 19, September 2005.
2. Lim, J.-S., C.-S. Kim, and D. Ahn, "Design of low-pass filters using defected ground structure," *IEEE Trans. on MTT*, Vol. 53, No. 8, 2005.
3. Fu, Y. Q. and N. C. Yuan, "Reflection phase and frequency bandgap characteristics of EBG structures with anisotropic periodicity," *Journal of Electromagnetic Waves and Applications*, Vol. 19, No. 14, 1897–1905, 2005.
4. Pendry, J. B., A. J. Holden, D. J. Robbins, and W. J. Stewart, "Magnetism from conductors and enhanced nonlinear phenomena," *IEEE Trans. on MTT*, Vol. 47, No. 11, 1999.
5. Burokur, S. N., M. Latrach, and S. Toutain, "Analysis and design of waveguides loaded with split-ring resonators," *Journal of Electromagnetic Waves and Applications*, Vol. 19, No. 11, 1407–1421, 2005.
6. Xu, W., L. W. Li, H. Y. Yao, T. S. Yeo, and Q. Wu, "Left-handed material effects on waves modes and resonant frequencies: filled waveguide structures and substrate-loaded patch antennas," *Journal of Electromagnetic Waves and Applications*, Vol. 19, No. 15, 2033–2047, 2005.
7. Mandal, M. K., P. Mondal, and A. Chakrabarty, "Low insertion Loss, sharp-rejection and compact microstrip low-pass filters," *IEEE Microwave and Wireless Component Letters*, Vol. 16, No. 11, 2006
8. Bonache, J., M. Gil, and J. Garcia-Garcia, "On the electrical characteristics of complementary metamaterial resonators," *IEEE Microwave and Wireless Component Letters*, Vol. 16, No. 10, 2006.